Axonal swellings predict the degeneration of epidermal nerve fibers in painful neuropathies

G. Lauria, MD; M. Morbin, MD, PhD; R. Lombardi, PhD; M. Borgna, PhD; G. Mazzoleni, PhD; A. Sghirlanzoni, MD; and D. Pareyson, MD

Abstract—*Objective:* To correlate the density of swellings in intraepidermal nerve fibers (IENF) with the longitudinal measurement of the epidermal innervation density in patients with painful neuropathy and to assess the predictive value of IENF swelling to progression of neuropathy. *Methods:* Fifteen patients with persistent pain in the feet underwent neurologic examination, nerve conduction studies, quantitative sensory examination, and skin biopsies at proximal thigh and distal leg. In all patients and in 15 healthy subjects, IENF density and swelling ratio (no. swellings/no. IENF) were quantified at distal leg. Follow-up study, including IENF density and swelling ratio quantification, was performed a mean of 19.2 months later. Double staining confocal microscope studies using anti-human protein-gene-product 9.5, anti-tubule, anti-neurofilament, and anti-synaptophysin antibodies were performed to assess specific accumulation within swellings. Ultrastructural investigation of IENF was also carried out. *Results:* Patients with neuropathy had lower density of IENF and higher swelling ratio than healthy subjects ($p < 0.01$) at distal leg. At follow-up, patients showed a parallel decrease in both IENF density ($p = 0.02$) and swelling ratio ($p = 0.002$). However, swelling ratio remained higher ($p = 0.03$) than in controls. Progression of neuropathy was confirmed by the decay in sural nerve sensory nerve action potential amplitude. Double immunostaining studies suggest accumulation of tubules and ubiquitin-associated proteins within swellings. Swollen and vacuolated IENF were identified in patients with neuropathy by conventional and immuno-electron microscopy. *Conclusions:* Increased swelling ratio predicted the decrease in IENF density in patients with painful neuropathy. Its quantification could support earlier diagnosis of sensory axonopathy.

NEUROLOGY 2003;61:631–636

Skin biopsy is used in the evaluation of painful neuropathies, to assess the predominant, or selective, impairment of unmyelinated sensory axons. The loss of intraepidermal nerve fibers (IENF), which are somatic axons, correlated with the presence and the severity of the neuropathy.[1–11] However, further criteria other than the simple count of IENF might be taken into account to increase the diagnostic yield of skin biopsy, mainly in patients with minimal or no evidence of neuropathy. Different studies[1,2,5,9] showed that in some patients, despite persisting positive sensory symptoms, IENF density at distal leg was within normal values. Patients with painful neuropathy frequently showed morphologic modifications of cutaneous nerves, such as periodic swellings of IENF, which were commonly considered degenerative changes.[2-5] Axonal swellings can occur in response to damage to the cytoskeleton and the transport systems[12,13] and could precede the loss of IENF.[14,15] In human painful neuropathies, they were never quantified and correlated to the course of the disease.

We assessed the swelling ratio of IENF (no. swellings/no. IENF) at distal leg in 15 patients with painful neuropathy and correlated it with the epidermal innervation density in a follow-up study. Results suggested that quantification of IENF swellings could strengthen the role of skin biopsy in the early diagnosis of sensory neuropathies.

Patients and methods. Fifteen patients (seven women; age 31 to 68 years) referred for persisting painful symptoms at the feet were examined. They underwent neurologic examination, nerve conduction studies (NCS), and quantitative sensory examination (QST) using the Computed-Assisted Sensory Examinator device (W.R. Medical Electronics Co., Stillwater, MN). Skin biopsies were taken at proximal thigh and distal leg in all patients and in 15 age-matched healthy subjects (9 women). Follow-up was carried out a mean of 19.2 months later (range 12 to 28 months). All patients and controls gave their informed consent to the study.

IENF density and swelling ratio quantification. Skin biopsies (3-mm punch; Stiefel Laboratories Ltd., Sligo, Ireland) were performed after local anesthesia with 2% lidocaine. Follow-up biopsies were taken from the same lower limb, close to the former one. Specimens were fixed in 2% paraformaldehyde-lysine-periodate for 24 hours at 4 °C, cryoprotected overnight, and serially cut with a freezing microtome to obtain 50-μm sections. Three sections were randomly selected from each biopsy and immunostained with polyclonal anti-human protein-gene-product 9.5 (PGP; Biogenesis Ltd., Poole, UK) as described.[3] Two observers (G.L. and M.B.), blinded to site and diagnosis, counted the total number of IENF in each section under a light microscope at high magnification, with the assistance of a microscope-mounted video camera. Individual fibers were counted as they crossed the dermal-

From the Department of Clinical Neuroscience (Drs. Lauria, Lombardi, Borgna, Sghirlanzoni, and Pareyson) and Section of Neuropathology (Drs. Morbin and Mazzoleni), National Neurological Institute "Carlo Besta," Milan, Italy.

Received December 4, 2002. Accepted in final form March 9, 2003.

Address correspondence and reprint requests to Dr. Giuseppe Lauria, Department of Clinical Neuroscience, National Neurological Institute "Carlo Besta," via Celoria, 11, 20133, Milan, Italy; e-mail: g_lauria@libero.it

Table *IENF density and swelling ratio in patients with painful neuropathy and age-matched healthy subjects*

			Baseline			Follow-up			Age-matched controls		
			IENF density			IENF density			IENF density		
Patient	Diagnosis	Neuropathic signs at baseline	Pth	Dl	Swelling ratio, Dl	Pth	Dl	Swelling ratio, Dl	Pth	Dl	Swelling ratio, Dl
1	Diabetes	+	12.7	6.0	0.60	11.5	3.0	0.26	27.0	12.5	0.29
2	Diabetes	+	26.0	5.2	0.83	22.0	3.9	0.72	21.5	9.0	0.31
3	Diabetes	+	20.7	4.7	0.54	18.0	3.6	0.51	32.6	14.2	0.26
4	Diabetes	+	15.0	5.9	0.55	13.5	4.1	0.32	28.5	10.7	0.23
5	Diabetes	+	27.9	11.4	0.62	23.4	6.8	0.50	25.1	16.4	0.22
6	Diabetes	+	12.7	5.0	0.43	10.5	0.0	0.00	13.5	15.9	0.13
7	Idiopathic	+	13.8	5.8	0.43	12.5	3.2	0.27	25.0	12.7	0.21
8	Idiopathic	+	18.9	6.6	0.57	17.7	3.4	0.48	18.2	10.4	0.16
9	AIDS	+	14.0	6.2	0.60	12.1	2.8	0.40	20.2	15.2	0.43
10	Taxol	−	13.1	8.3	0.54	12.3	5.4	0.36	15.6	11.8	0.30
11	Idiopathic	−	10.1	3.2	0.61	10.0	2.3	0.59	22.0	18.0	0.56
12	Idiopathic	−	22.0	18.0	0.55	19.6	13.0	0.45	25.2	16.1	0.46
13	Idiopathic	−	25.5	13.5	0.68	21.1	6.4	0.59	21.1	19.1	0.42
14	Idiopathic	−	30.4	17.3	0.64	28.0	9.0	0.38	21.9	18.2	0.22
15	Idiopathic	−	13.5	8.9	0.72	12.6	6.2	0.52	21.9	15.4	0.32
Mean (SD)			18.4 (6.5)	8.4 (4.6)	0.59 (0.1)	16.3 (5.5)	4.9 (3.1)	0.42 (0.2)	22.6 (4.8)	14.4 (3.0)	0.30 (0.12)

Neuropathic signs included reduced or absent Achilles tendon reflexes and reduced light-touch and pinprick sensation at distal lower extremities.

IENF = intraepidermal nerve fibers; Pth = proximal thigh; Dl = distal leg; Swelling ratio = no. swellings/no. IENF (mean of three values calculated at distal leg).

epidermal junction; secondary branching within the epidermis was excluded from the quantification. The length of the epidermis was measured using a computerized system (Microscience Inc., Seattle, WA) and the linear density of IENF (IENF/mm) obtained.

Swelling ratio of IENF (no. of swellings/no. of IENF) at distal leg was calculated at both first examination and follow-up in the same three sections in which IENF density was previously quantified by the same blinded observers. All IENF swellings with a diameter above 1.5 μm were counted, whereas enlargements below this value were considered normal axonal varicosity and excluded from the quantification. Terminal enlargements of IENF were a priori excluded from quantification. A 1.5-μm–length marker was constantly kept on the upper right corner of the monitor to check the diameter of swellings. Individual IENF density and swelling ratio were compared using the two-tailed Student *t*-test. Interobserved agreement was assessed by the Spearman correlation coefficient.

Confocal microscope studies. Double immunofluorescence studies were performed using polyclonal anti-PGP antibodies and each of the following monoclonal antibodies: anti-unique β-tubulin (TuJ1, Berkley Antibody Company, Richmond, CA), anti-microtubule-associated protein-1B (MAP-1B, Roche Diagnostics Corp., Indianapolis, IN), anti-neurofilament (NF, Dako, Glostrup, Denmark), anti-phosphorylated neurofilament (SMI 312, Sternberger Monoclonals Incorporated, Baltimore, MD), and anti-synaptophysin (Dako, Glostrup, Denmark).

Sections were preincubated for 1 hour in 0.1 M phosphate buffered saline (PBS) containing 1% bovine serum albumin (BSA, Sigma Chemical Co., St. Louis, MO) and 0.4% Triton X-100. Primary antisera (PGP 1:500, TuJ1 1:1000, MAP-1B 1:100, NF 1:100, SMI 312 1:200, synaptophysin 1:10) were added with 0.1% BSA in 0.1 M PBS and incubated for 2 nights at 4 °C. Cy2-conjugated immunoglobulin G (IgG) goat antirabbit (H+L) (AffiniPure, Jackson Immuno Research Laboratories, Inc., West Grove, PA) was used as secondary antibody for polyclonal PGP. Biotinylated horse antimouse IgG (H+L) (Vector Laboratories, Inc., Burlingame, CA) was used as secondary antibody for monoclonal TuJ1, MAP-1B, NF, SMI 312, and synaptophysin, followed by amplification with rhodamine Red-X-conjugated streptavidin (Jackson Immuno Research Laboratories, Inc.). Samples were viewed using appropriate filters with a MicroRadiance 2000 Confocal Imaging System (Bio-Rad, Hemel Hempstead, UK) and a Nikon 600 fluorescence microscope (Melville, NY). Each image was collected in successive frames of 0.5 to 1 μm apart at 40× magnification and was integrated by a computerized system (LaserSharp 2000; Bio-Rad).

Conventional electron microscope study. Specimens were fixed in 2.5% EM grade glutaraldehyde (Fluka Chemie, AG Buchs, CH) in 0.05 M PBS at pH 7.4, postfixed in 1% osmium tetroxide (Electron Microscopy Sciences, Fort Washington, PA) in 0.05 M PBS, dehydrated in graded acetone, and embedded in Spurr (EMS). Thin sections (500 Å thick) of selected areas including dermal-epidermal junction were harvest on 200 mesh copper grids (EMS) stained with lead citrate and uranyl acetate and viewed with a Zeiss EM 109 electron microscope.

Immuno-electron microscope study. Specimens were fixed in 0.04% (w/v) paraformaldehyde (BDH Italia, Milan, Italy) plus 1% glutaraldehyde for 3 hours and in 0.6% glutaraldehyde overnight, dehydrated in graded acetone, and embedded in Spurr. Thin sections of selected areas including dermal-epidermal junction were collected on formvar-carbon coated 200 mesh nickel grids (EMS) and processed using the following protocol: 1 hour incubation in 1% Na periodate, dip in 0.05 M glycine pH 4.0 (Sigma, St Louis, MO), and cover with Aurion-BSA incubation buffer (Aurion, Wageningen, the Netherlands) for 30 minutes. Polyclonal anti-PGP antibody was diluted 1:100 in the same buffer and placed on grids overnight at 4 °C. Following wash in Aurion-BSA, grids were incubated with goat antirabbit gold (GAR-10) conjugated antibody (Aurion) diluted 1:20 in PBS for 3 hours at room temperature. Sections were fixed in 1% glutaraldehyde, postfixed in 1% OsO_4, and counterstained with uranyl acetate and lead citrate.

Results. *Clinical findings.* All patients had burning feet or pain bilaterally involving distally the lower extrem-

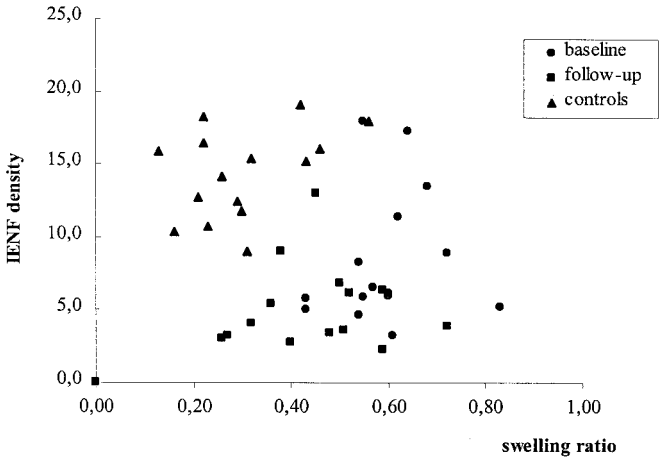

Figure 1. Relationship between intraepidermal nerve fiber (IENF) density and swelling ratio at the distal leg in patients with painful neuropathies at baseline and follow-up and in age-matched healthy subjects.

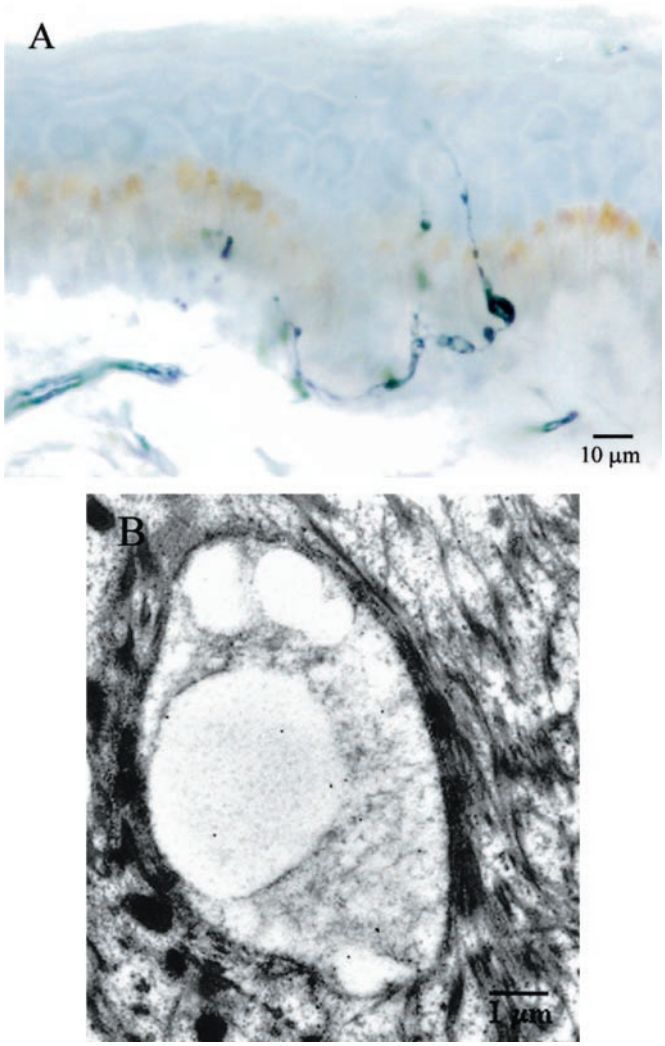

Figure 2. (A) Light microscope protein-gene-product 9.5 (PGP) immunostaining shows an intraepidermal nerve fiber (IENF) with multiple swellings, which appeared partly or completely vacuolated. (B) PGP immuno-electron microscope image shows a swollen IENF with amorphous debris and several vacuoles. Note the 10-nm gold particles within the structure.

ities for a mean of 2.5 years (range 0.5 to 4 years). Neuropathy was related to diabetes in six patients, to AIDS in one patient, and to Taxol toxicity in one patient; it was idiopathic in seven patients. At the first evaluation, nine patients showed reduced or absent Achilles tendon reflexes, decreased light touch and pinprick sensation at distal lower extremities, and mean sural sensory nerve action potential (SNAP) amplitude of 6.2 ± 3.5 μV. The other six patients (five idiopathic and Taxol-associated neuropathy) had normal results on neurologic examination and higher ($p = 0.01$) sural SNAP amplitude (15.9 ± 5.5 μV). Results of strength and motor nerve conduction studies were normal in all patients. Vibratory threshold was increased (>99th percentile) in all except one patient who had 94th percentile, whereas cooling threshold was increased in only five patients.

At follow-up, all patients had a worsening of symptoms and showed a decrease ($p = 0.04$) in sural SNAP amplitude (6.7 ± 6.6 μV). This was more evident in patients who had signs of neuropathy at the first observation (1.9 ± 3.3 μV) than in those without (9.9 ± 6.5 μV). Vibratory threshold was increased in all patients, whereas cooling threshold was >99th percentile in eight of them. In two of the six patients with normal clinical picture at baseline (one idiopathic and Taxol-associated neuropathy), reduced Achilles tendon reflexes and slight decrease of light touch and pinprick sensation at distal lower extremities were observed.

IENF density quantification. At the first examination, IENF density at distal leg was lower ($p < 0.01$) in patients than in healthy subjects (8.4 ± 4.6/mm and 14.4 ± 3.0/mm), whereas it did not differ at proximal thigh (18.4 ± 6.5/mm and 22.6 ± 4.8/mm; $p = 0.05$). Patients with signs of neuropathy showed a lower IENF density at distal leg than those without (6.3 ± 2.0/mm and 11.5 ± 5.7/mm; $p = 0.04$). At follow-up, patients showed a decrease in IENF density also at proximal thigh, which became lower than in healthy subjects. Compared with baseline, density at distal leg was lower (4.9 ± 3.1/mm; p = 0.02), whereas the difference was not significant at proximal thigh (16.3 ± 5.5/mm; $p = 0.3$) (table).

Swelling ratio quantification. Swelling ratio of IENF at distal leg was higher ($p < 0.001$) both in patients with neuropathic signs (0.57 ± 0.12) and in those without (0.62 ± 0.07) than in healthy subjects (0.30 ± 0.12). Moreover, it was also higher in Patients 12 through 15, who showed normal IENF density at the first examination (see the table). At follow-up, patients showed a lower swelling ratio (0.42 ± 0.17; $p = 0.002$) than that found at the first observation, although the value remained higher ($p = 0.03$) than in controls (figure 1). Spearman correlation coefficient was 0.88 ($p < 0.01$), indicating a high inter-observed agreement in swelling quantification.

Morphologic findings. In patients, the diameter of IENF swellings ranged between 1.8 and 5.4 μm. Some swellings showed a nonhomogeneous PGP labeling, whereas others appeared partly or completely vacuolated (figure 2). In healthy subjects, IENF often showed fine varicosities and club-like endings.

In both healthy subjects and patients, double staining confocal microscope studies disclosed that both TuJ1 and

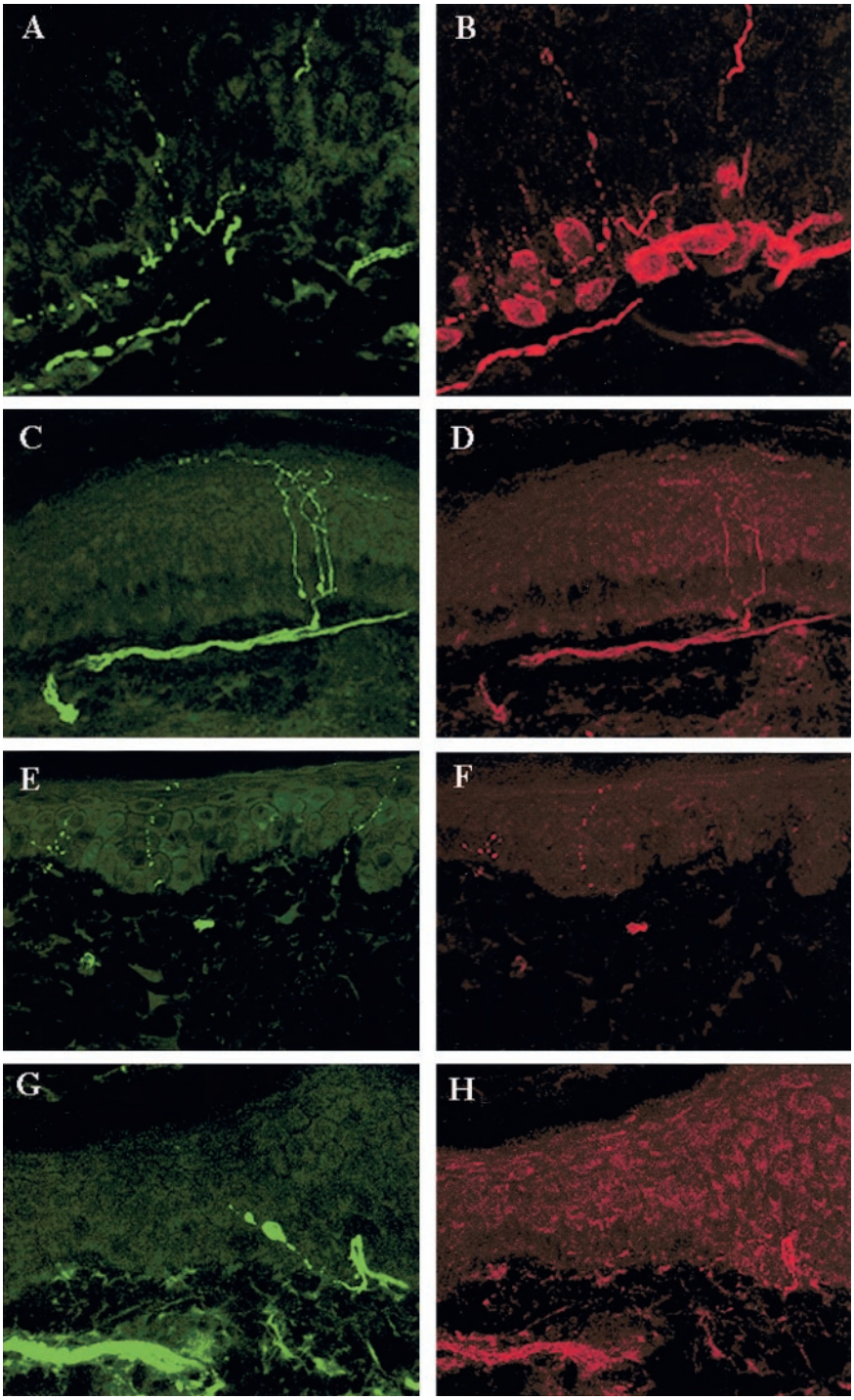

Figure 3. Confocal microscope double staining colocalization studies (40× objective) between protein-gene-product 9.5 (PGP) (A, C, E, and G) and β-tubulin (B), microtubule-associated protein-1B (MAP-1B, D), neurofilament (F), and anti-synaptophysin (H) in skin biopsies taken at the distal leg in patients with neuropathy. Note the colocalization between PGP and MAP-1B (D) through the length of the fibers, but not within the swellings. Synaptophysin (H) did not stain intraepidermal nerve fiber swellings.

MAP-1B diffusely colocalized with PGP in IENF, whereas NF and SMI 321 were expressed in fewer epidermal axons. Similarly, almost all PGP-positive swellings presented immunoreactivity to TuJ1, whereas fewer showed NF labeling. Swellings did not present immunoreactivity to synaptophysin, which was observed only in some dermal nerve fibers (figure 3). Other PGP-positive processes were identified within the epidermis, including faint staining of Langerhans cell processes, which, however, showed intense TuJ1 staining.

Single membrane-bound profiles containing few identifiable organelles, such as mitochondria, vesicles, and tubular structures of 10 to 20 nm, likely representing axonal profiles, were observed within all the epidermal vital layers in both controls and patients with neuropathy by conventional electron microscopy. However, only these profiles showed PGP immunoreactivity on immuno-electron microscopy. In patients with neuropathy, swollen axons with granular disintegration of the cytoskeleton and vacuoles could be observed (see figure 2).

Discussion. The availability of antibodies against the panaxonal marker PGP allowed demonstration and quantification of the extensive innervation of the

epidermis by sensory unmyelinated axons.[16] Several studies, including the current one, demonstrated the correlation between the decrease in IENF density and the severity of neuropathy.[1-10]

We aimed at strengthening the role of skin biopsy in the diagnosis of painful neuropathies by quantifying the swelling ratio of IENF at distal leg, beside the epidermal innervation density. In fact, periodic swellings of IENF, which were considered degenerative changes,[17] were never before quantified or correlated to the course of the neuropathy. This could be useful in identifying early sensory axonopathy in patients with persistent painful symptoms at the feet, particularly in those showing normal IENF count.

We found that swelling ratio of IENF at distal leg was significantly higher in patients with neuropathy than in healthy subjects, indicating an increased number of axons with likely degenerative changes. This was also observed in four patients with persistent burning feet and normal IENF density at the first examination (Patients 12 through 15). The hypothesis that diffuse swellings might represent early evidence of IENF axonopathy was supported by the results of follow-up examination. In fact, all patients showed a decrease in epidermal innervation density at distal leg (see the table), suggesting that swellings preceded the eventual loss of IENF. Moreover, at follow-up we found a decrease in swelling ratio, which appeared to have a linear relationship with the decrease in IENF density, although the value remained significantly higher than that in healthy subjects (see figure 1). Progression of neuropathy was also confirmed by the decrease in sural SNAP amplitude at follow-up evaluation.

These findings appeared in keeping with the results of recent experimental studies that demonstrated that swellings of IENF occurred very early after sciatic nerve axotomy[14] and acrylamide intoxication,[15] and predicted their disappearance. Several factors, including toxic agents, diabetes, and ischemia, can influence the caliber of axons leading to failure in the axonal transport systems and derangement of the cytoskeleton.[12] Accumulation of neurofilaments and microtubules, followed by their degradation into amorphous debris, can result in the formation of axonal swellings.[13,14,18,19]

In healthy subjects, IENF typically showed tiny varicosity, which likely reflected the uneven distribution of cytoskeletal components. Normal IENF often ended with a single club-like enlargement, as previously described.[6] For this reason, we excluded a priori terminal enlargements from swelling ratio quantification. In patients with neuropathy, the diameter of swellings was two- to fivefold that of normal axons. They showed intense, although not always homogeneous, PGP staining, and could be partly or completely vacuolated, suggesting different stages of axonal degeneration (see figure 2). Fragmented and discontinuous dermal nerve bundles were also usually observed in patients with neuropathy. Confocal double staining studies were performed to identify accumulation of specific cytoskeletal components within IENF swellings. In healthy subjects, almost all IENF coexpressed PGP, TuJ1, and MAP-1B, whereas fewer IENF showed NF labeling. Similarly, in patients with neuropathy, PGP and TuJ1 colocalized in most swollen IENF, whereas fewer axons showed immunoreactivity to NF. These findings suggested that tubules were the main component of IENF cytoskeleton and that they accumulated with ubiquitin-associated proteins within swellings. Conversely, vesicles did not appear to accumulate within swellings, as suggested by the absence of immunoreactivity to synaptophysin (see figure 3).

Langerhans cell processes showed faint PGP staining and intense TuJ1 labeling. Moreover, epidermal axons are single membrane bound, because Schwann cell ensheathment ends at the dermal-epidermal junction.[3] These were major limitations for ultrastructural investigation of nerve fibers within the epidermis, which required extensive evaluation of several sections. However, axon profiles were detected within all the epidermal layers in controls and patients with neuropathy. They were between keratinocytes or in membrane apposition with them, as previously shown by other authors.[20,21] In swollen IENF, axoplasm was mainly replaced by amorphous debris. In patients with neuropathy, several IENF showed one or more vacuoles, which likely corresponded to the areas of nonhomogeneous PGP staining observed under light microscopy (see figure 2).

References

1. Periquet MI, Novak V, Collins MP, et al. Painful sensory neuropathies. Prospective evaluation using skin biopsy. Neurology 1999;53:1641–1647.
2. Holland NR, Stocks A, Hauer P, et al. Intraepidermal nerve fiber density in patients with painful sensory neuropathy. Neurology 1997;48:708–711.
3. McCarthy BG, Hsieh ST, Stocks A, et al. Cutaneous innervation in sensory neuropathies: evaluation by skin biopsy. Neurology 1995;45:1848–1855.
4. Kennedy WR, Wendelschafer-Crabb G, Johnson T. Quantitation of epidermal nerves in diabetic neuropathy. Neurology 1996;47:1042–1048.
5. Holland NR, Crawford TO, Hauer P, et al. Small-fiber sensory neuropathies: clinical and neuropathology of idiopathic cases. Ann Neurol 1998;44:47–59.
6. Lauria G, Holland N, Hauer P, et al. Epidermal innervation: changes with aging, topographic location, and in sensory neuropathy. J Neurol Sci 1999;164:172–178.
7. Chien HF, Tseng TJ, Lin WM, et al. Quantitative pathology of cutaneous nerve terminal degeneration in the human skin. Acta Neuropathol 2001;102:455–461.
8. Smith GA, Ramachandran P, Tripp S, Singleton RJ. Epidermal nerve innervation in impaired glucose tolerance and diabetes-associated neuropathy. Neurology 2001;57:1701–1704.
9. Herrmann DN, Griffin JW, Hauer P, et al. Epidermal nerve fiber density and sural nerve morphometry in peripheral neuropathies. Neurology 1999;53:1634–1640.
10. Polydefkis M, Yiannoutsos CT, Cohen BA, et al. Reduced intraepidermal nerve fiber density in HIV-associated sensory neuropathy. Neurology 2002;58:115–119.
11. Nolano M, Simone DA, Wendelschafer-Crabb G, et al. Topical capsaicin in humans: parallel loss of epidermal nerve fibers and pain sensation. Pain 1999;81:135–145.
12. Hoffman PN, Griffin JW. The control of axonal caliber. In: Dyck PJ, Thomas PK, Griffin JW, Low PA, Poduslo JF, eds. Peripheral neuropathy. Philadelphia: WB Saunders, 1993:389–400.
13. Tanner KD, Levine JD, Topp KS. Microtubule disorientation and axonal swelling in unmyelinated sensory axons during vincristine-induced painful neuropathy in rat. J Comp Neurol 1998;395:481–492.
14. Hsieh ST, Chiang HY, Lin WM. Pathology of nerve terminal degeneration in the skin. J Neuropathol Exp Neurol 2000;59:297–307.
15. Ko MH, Chen WP, Hsieh ST. Cutaneous nerve degeneration induced by acrylamide in mice. Neurosci Lett 2000;293:195–198.

16. McArthur JC, Stocks AE, Hauer P, et al. Epidermal nerve fiber density. Normative reference range and diagnostic efficiency. Arch Neurol 1998; 55:1513–1520.
17. Kennedy WR, Said G. Sensory nerves in skin. Answers about painful feet? Neurology 1999;53:1614–1615.
18. Schmidt RE, Dorsey D, Parvin CA, et al. Dystrophic axonal swellings developed as a function of age and diabetes in human dorsal root ganglia. J Neuropathol Exp Neurol 1997;56:1028–1043.
19. Griffin JW, Hoffman PN. Degeneration and regeneration in the peripheral nervous system. In: Dyck PJ, Thomas PK, Griffin JW, Low PA, Poduslo JF, eds. Peripheral neuropathy. Philadelphia: WB Saunders, 1993:361–372.
20. Hilliges M, Wang L, Johansson O. Ultrastructural evidence for nerve fibers within all vital layers of the human epidermis. J Invest Dermatol 1995;104:134–137.
21. Kennedy WR, Wendelschafer-Crabb G. The innervation of human epidermis. J Neurol Sci 1993;115:184–190.

CME

Temporal lobe tumoral epilepsy

Characteristics and predictors of surgical outcome

Megdad M. Zaatreh, MD; Katrina S. Firlik, MD; Dennis D. Spencer, MD; and Susan S. Spencer, MD

Abstract—*Objective:* To review the clinical and neurophysiologic features and surgical outcome in patients with intractable temporal lobe tumoral epilepsy. *Methods:* Patients with intractable temporal lobe epilepsy who underwent resection of temporal lobe tumors, confirmed by surgical pathology, seen between 1985 and 2000 at Yale University School of Medicine Epilepsy Center, were selected. Medical records were reviewed for age at diagnosis, age at onset of seizures, delay between seizure onset and tumor diagnosis, types and frequencies of seizures, EEG results, use of anticonvulsants, extent of surgery, and pathologic diagnosis. *Results:* Sixty-eight patients were identified, 94.1% of them with low-grade tumors. Complex partial seizure was the most common seizure type. All patients underwent at least one surgical procedure with average follow-up of 9 years after surgical intervention. Eighty-seven percent of patients had significant postoperative seizure improvement (Engel's classes I and II). Gross total tumor resection predicted postoperative seizure freedom ($p = 0.002$), whereas patients with early surgical intervention, auras, and simple partial seizures had a tendency toward better seizure outcome. *Conclusions:* Long-term follow-up of patients with intractable temporal lobe tumoral epilepsy suggests good response of seizures to surgery, which is unrelated to age at diagnosis, EEG, or pathology. Extent of tumor resection was significantly predictive of outcome, whereas early intervention and presence of simple partial seizures showed trends as predictive factors.

NEUROLOGY 2003;61:636–641

Chronic epilepsy due to brain tumors has been described since the nineteenth century,[1] and multiple studies have addressed various aspects of tumoral epilepsy.[2-4] The remarkable advances in neuroimaging techniques now allow detection of previously unknown tumors, so new scrutiny is warranted.[5] Pathophysiology of tumoral epilepsy is poorly understood and may be related to biochemical, anatomic, and physiologic changes, especially in the peritumoral tissue, which seems to be the major source of seizure generation.[6-8] The best approach to management of tumoral epilepsy is controversial in some cases, although resective surgery is often advocated.[9]

Temporal lobe resection is the most common surgical treatment in refractory epilepsy, with robust evidence supporting the safety and efficacy of this procedure.[10,11] Numerous publications reported predictors of surgical outcomes and long-term prognosis in patients with temporal lobe epilepsy, though in most studies, emphasis was placed on patients with mesial temporal sclerosis, with few temporal neoplasms represented.[11,12] Yet most chronic epilepsy associated with tumors is also temporal in origin. Few studies addressed the clinical, electrographic, and surgical features of temporal lobe epilepsy specifically associated with tumor.[13,14] We report our experience with temporal lobe tumoral epilepsy with special attention to the clinical aspects, presurgical diagnostic workup, and long-term surgical outcomes.

Methods. *Patient selection.* Medical records of all patients with medically intractable partial epilepsy who underwent resection of temporal lobe tumors (confirmed by surgical pathology) seen between January 1985 and July 2000 at Yale University School of Medicine Epilepsy Center were reviewed. Data collected included age at tumor diagnosis, age at onset of seizures, delay between seizure onset and tumor diagnosis, other seizure risk factors, types and frequencies of seizures, EEG results, use of anticonvulsants, extent of surgery, and pathologic diagnosis. Patients with <2 years follow-up, incomplete data, neurocutaneous disorders, or prior brain surgery were excluded.

Patient evaluation. All patients were diagnosed using preoperative high-resolution brain MRI. Prior to surgery, identification of the epileptic zone was attempted using most or all of the following: clinical seizure semiology, scalp interictal EEG localization,

From the Departments of Neurology (Drs. Zaatreh and S.S. Spencer) and Neurosurgery (Drs. Firlik and D.D. Spencer), Yale University School of Medicine, New Haven, CT.

Received February 28, 2003. Accepted in final form May 14, 2003.

Address correspondence and reprint requests to Dr. S.S. Spencer, Department of Neurology, Yale University School of Medicine, P.O. Box 208018, New Haven, CT 06520-8018; e-mail: susan.spencer@yale.edu

